Solving the Cauchy Problem Related to the Helmholtz Equation through a Genetic Algorithm

JAMAL DAOUDI[1], CHAKIR TAJANI[2*]
[1,2] SMAD Team, Department of Mathematics
Polydisciplinary Faculty of Larache
Abdelmalek Essaadi University
MOROCCO

Abstract: - The Cauchy problem associated with the Helmholtz equation is an ill-posed inverse problem that is challenging to solve due to its instability and sensitivity to noise. In this paper, we propose a metaheuristic approach to solve this problem using Genetic Algorithms in conjunction with Tikhonov regularization. Our approach is able to produce stable, convergent, and accurate solutions for the Cauchy problem, even in the presence of noise. Numerical results on both regular and irregular domains show the effectiveness and accuracy of our approach.

Key-Words: - Inverse Problem, Helmholtz Equation, Tikhonov Regularization, Optimization, Genetic Algorithms

Received: May 19, 2023. Revised: August 21, 2023. Accepted: September 27, 2023. Published: October 9, 2023.

1 Introduction

Let $\mathbf{\Omega}$ be an open and bounded domain in $\mathbb{R}^2$ with a smooth boundary Γ. We divide the boundary into two disjoint parts, $\Gamma = \Gamma_i \cup \Gamma_c$, where $\Gamma_i \cap \Gamma_c = \emptyset$ and $\mathrm{mes}(\Gamma_c) \neq 0$.

Mathematical formulation of the Cauchy problem for the Helmholtz equation can be expressed as:

$$(P): \begin{cases} -\Delta u + \kappa^2 u = 0 & \text{in} \quad \Omega \\ u = f & \text{on} \quad \Gamma_c \\ \partial_n u = g & \text{on} \quad \Gamma_c \end{cases} \tag{1}$$

where Δ is the Laplacian operator, ∂_n denotes the outward normal derivative, κ is a complex number (wave number), f and g are the Cauchy data available on the accessible boundary Γ_c.

This problem arises in many important physical applications related to wave propagation and vibration phenomena see, [1], [2], [3], [4].

The Helmholtz equation is a fundamental equation in physics that describes the propagation of waves. In the past century, extensive research has been carried out on the direct problem of the Helmholtz equation, which involves finding the solution to the equation given boundary data (Dirichlet, Neumann and Dirichlet-Neumann). However, in practical situations, it is often not possible to obtain boundary data for the entire boundary. Instead, we may only have access to noisy data related to a specific section of the boundary or some points within the domain. This leads to inverse problems, in which the goal is to find the solution to the equation given incomplete or noisy data.

The Cauchy problem for the Helmholtz equation is an example of an inverse problem that is ill-posed. This means that small perturbations in the given data can result in significant changes to the solution, and the solution does not continuously depend on the given Cauchy data. This makes it difficult to find accurate solutions to the Cauchy problem, and special methods are often required. References, [5], and, [6], discuss the ill-posedness of the Cauchy problem for the Helmholtz equation in more detail. Conventional numerical methods are not sufficient for solving the problem being investigated. To remedy this, numerous numerical methods have been suggested in order to solve the Cauchy problem for the Helmholtz equation, such as the method of fundamental solution, [7], the method of plane waves, [8], the Landweber approach, [9], the method of Fourier regularization, [10], [11], conjugate gradient method, [12], [13], the boundary element minimal error method, [14], the method of spherical wave expansion, [15], the method of boundary knot, [16].

For solving the Cauchy problem associated with the Helmholtz equation, two main approaches are commonly used: iterative methods and direct methods. Iterative methods start with an initial guess of the solution and then iteratively improve the guess by minimizing a cost function, such as the error between the calculated and measured data. This process can be computationally intensive, as the problem must be solved at each iteration. However, iterative methods are often more robust than direct methods and can be used to solve problems that are ill-posed. On the other hand, direct methods require less computational time as the problem is discretized only once, but they may be susceptible to numerical instability.

It should be noted that the aforementioned methods are deterministic techniques, However, deterministic approach has limitations, particularly when dealing with complex systems that are influenced by many variables and factors. In such cases, deterministic models may not be able to account for all the variables and uncertainties involved, leading to inaccuracies and incomplete understanding of the system. Beside deterministic techniques, there is a second class called stochastic techniques. Stochastic techniques refer to a class of mathematical methods that deal with randomness, uncertainty, and probability.

Metaheuristic algorithms draw inspiration from natural processes such as biological evolution, swarm intelligence, and other phenomena. For instance, genetic algorithms, [17], emulate natural selection and evolution, while particle swarm optimization, [18], mimics the collective behavior of flocks of birds or swarms of insects. Similarly, ant colony optimization, [19], is based on the behavior of real ant colonies, and the bat algorithm, [20], imitates the echolocation behavior of bats. These algorithms are designed to efficiently explore a vast search space by iteratively generating and evaluating candidate solutions, with the goal of finding an optimal or near-optimal solution.

This study proposes a new computational algorithm for solving the Cauchy problem related to the Helmholtz equation. The method is based on a genetic algorithms coupled with Tikhonov Regularization, and considers the solution on the underspecified Γ_i boundary as a control in a direct mixed well-posed problem. The proposed approach aims at accurately fitting the Cauchy data on the overspecified boundary Γ_c by minimizing a cost function that measuring the discrepancies between the available data and the corresponding calculated values.

The rest of this paper is outlined as follows. Section 2 introduces the formulation of the inverse problem under consideration. In Section 3, we offer a concise overview of genetic algorithms and explore the capabilities of the real-coded genetic algorithms, which has been tailored to solve the inverse problem under consideration. To demonstrate the accuracy and efficiency of the proposed method, Section 4 presents two numerical examples featuring regular and irregular domains. Finally, Section 5 summarizes the key findings of the research and offers concluding remarks.

2 Formulation of the problem as an optimization problem

2.1 Optimization problem

The purpose of this paper is the use an adapted genetic algorithm with real coded combined with finite element method to estimate the Cauchy data on the inaccessible part of the boundary Γ_i from the available data f and g on Γ_c.

Since the ϕ and ϕ' on the boundary Γ_i is to be determined, two direct problems are considered:

$$(P_D): \begin{cases} -\Delta u + \kappa^2 u = 0 & \text{in} \quad \Omega \\ u = \phi & \text{on} \quad \Gamma_i \\ \partial_n u = g & \text{on} \quad \Gamma_c \end{cases} \tag{2}$$

$$(P_N): \begin{cases} -\Delta u + \kappa^2 u = 0 & \text{in} \quad \Omega \\ u = f & \text{on} \quad \Gamma_c \\ \partial_n u = \phi' & \text{on} \quad \Gamma_i \end{cases} \tag{3}$$

It should be noted that if $\phi \in H^{1/2}(\Gamma_i)$ and $g \in H^{-1/2}(\Gamma_c)$ (resp $f \in H^{1/2}(\Gamma_c)$ and $\phi' \in H^{-1/2}(\Gamma_c)$), then there is a unique solution $u(\phi, g)$ (resp $u(\phi', f)$) of the direct problem Eq.(2) (resp Eq.(3)) see, [21], and we are looking for ϕ (resp ϕ') such that:

$$\begin{cases} u(\phi, g) = f & \text{on} \quad \Gamma_c \\ \partial_n u(\phi', f) = g & \text{on} \quad \Gamma_c \end{cases} \tag{4}$$

which leads to minimize the least-squares functional $\mathcal{J}_\mathcal{D}$ and $\mathcal{J}_\mathcal{N}$ defined by:

$$\mathcal{J}_\mathcal{D}(\phi) = \frac{1}{2}\|u(\phi, g) - f\|^2_{L^2(\Gamma_c)} \tag{5}$$

and

$$\mathcal{J}_\mathcal{N}(\phi') = \frac{1}{2}\|u(\phi', f) - g\|^2_{L^2(\Gamma_c)} \tag{6}$$

2.2 Tikhonov regularization

In an inverse problem, the observed data is typically affected by noise and measurement errors, which can lead to instability and poor accuracy in the estimation of the unknown parameters. Tikhonov regularization helps to overcome these issues by introducing a regularization term.

In this case the Tikhonov regularization method is used to convert the tow objective functions Eq.(5) and Eq.(6) to the well-posed form given as follows:

$$\mathcal{J}_{\mathcal{DR}}(\phi) = \frac{1}{2}\|u(\phi, g) - f\|^2_{L^2(\Gamma_c)} + \frac{\alpha}{2}\|\phi\|^2_{L^2(\Gamma_i)} \quad (7)$$

and

$$\mathcal{J}_{\mathcal{NR}}(\phi') = \frac{1}{2}\|u(\phi', f) - g\|^2_{L^2(\Gamma_c)} + \frac{\beta}{2}\|\phi'\|^2_{L^2(\Gamma_i)} \quad (8)$$

where α and β are the regularization parameters, $\frac{\alpha}{2}\|\phi\|^2$ and $\frac{\beta}{2}\|\phi'\|^2$ are the well-known Tikhonov regularization terms. In the literature, there are various effective techniques recommended for choosing the most suitable value for the regularization parameter, including the L-curve method, [22], and the discrepancy principle, [23]. These approaches avoid the need to use excessively small or large positive values of α (resp β) to assure the stability of the solution.

3 Application of genetic algorithms to inverse problem

3.1 Overview of genetic algorithms

Genetic algorithms, [24], have proven to be effective in solving a variety of optimization problems. They are based on the principles of biological evolution and operate as a searching method. A population of chromosomes is used to represent potential solutions and genetic operators are applied to progressively improve each chromosome, which becomes the basis for the next generation. This process continues until the desired number of generations has been completed or a predefined stopping criteria value has been reached.

Genetic algorithms offer a number of advantages over other optimization approaches. First, they search from a population of solutions instead of just one. Second, they can use any fitness function, even if it is not continuous. Third, they use random operators to generate new solutions. Fourth, they do not need to know anything about the problem to find a good solution.

Genetic algorithms typically consist of the following basic elements:

1. Initialization: The genetic algorithm begins by creating a population of potential solutions to the problem being solved. This is typically done by randomly generating a set of individuals, where each individual is a potential solution represented as a set of genes or chromosomes.

2. Fitness function: The fitness function is used to evaluate each individual in the population and assign a fitness score based on how well it solves the problem being considered. The fitness score is used to select individuals for reproduction in the next generation.

3. Selection: The selection process involves choosing the fittest individuals from the current generation to be parents for the next generation. The individuals are selected using various techniques such as roulette wheel selection or tournament selection.

4. Crossover: Crossover is the process of combining genetic material from two parents to create a new individual in the next generation. This is typically done by selecting two parents based on their fitness score and swapping genetic material between them to create a new individual.

5. Mutation: Mutation introduces random changes to the genetic material of an individual, leading to potentially new and improved solutions. It is typically applied to a small fraction of individuals in the population to maintain genetic diversity.

6. Termination: The algorithm terminates when a stopping criterion is met, such as reaching a desired fitness score or running for a certain number of generations.

We can summarize these steps in the following diagram, Fig.1.

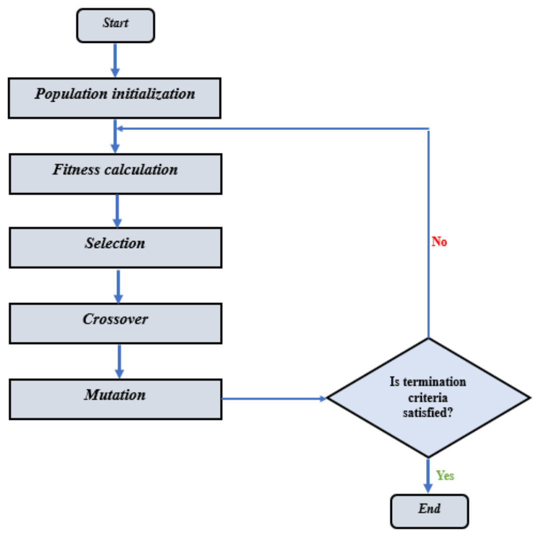

Figure 1: Flowchart of genetic algorithms.

These elements work together to produce a population of increasingly fit individuals that can be used to find optimal solutions to a wide range of problems.

3.2 Genetic operators

In order to address the Cauchy problem associated with the Helmholtz equation, we consider a real coded (floating-point) GAs (RCGA), which perform better than binary coded GA, where the chromosome corresponds to a vector of real parameters, the gene corresponds to a real number, and the allele corresponds to a real value.

3.2.1 Crossover

This operator is the most important operator in the genetic process between two individuals selected according to a probability p_c, [25], [26], producing new offspring. Several crossover operators have been developed, adapted to the type of encoding used. In this study, we consider the arithmetic crossover operator with real encoding.
Typically, parents are denoted as:

$$\begin{aligned} Par^{(1)} &= \left(Par_1^{(1)}, \ldots, Par_n^{(1)}\right) \\ Par^{(2)} &= \left(Par_1^{(2)}, \ldots, Par_n^{(2)}\right) \end{aligned} \tag{9}$$

The representation of offspring is given by:

$$\begin{aligned} Off^{(1)} &= \left(Off_1^{(1)}, \ldots, Off_n^{(1)}\right) \\ Off^{(2)} &= \left(Off_1^{(2)}, \ldots, Off_n^{(2)}\right) \end{aligned} \tag{10}$$

where, $Off^{(i)}$ and $Par^{(j)}$ represent the i^{th} offspring and j^{th} parent, respectively. The variable n denotes the number of genes on each individual.

In arithmetic crossover two parents produce two offspring which can be expressed using Eq.(11) given as follows:

$$\begin{aligned} Off_i^{(1)} &= \alpha_i Par_i^{(1)} + (1-\alpha_i)\, Par_i^{(2)} \\ Off_i^{(2)} &= \alpha_i Par_i^{(2)} + (1-\alpha_i)\, Par_i^{(1)} \end{aligned} \tag{11}$$

where, α_i represents uniformly distributed random numbers.
It is important to mention that α_i can be generated at each generation; in this case we talk about non-uniform arithmetic crossover, [27].

3.2.2 Mutation

The mutation operator is applied to specific elements of selected chromosomes. If we consider the selected chromosome at the k^{th} generation, in the following form:

$$Off = (Off_1, \ldots, Off_i, \ldots, Off_n)$$

the form of the obtained chromosome, knowing that Off_i is the element to be mutated, is given by:

$$Off' = (Off_1, \ldots, Off_i', \ldots, Off_n)$$

Non-uniform mutation is one of the commonly used mutation operators in real-coded genetic algorithms (RCGAs), [28], [29]. It is defined as follows:

$$Off_i' = \begin{cases} Off_i + \delta\left(k, u_i - Off_i\right), & \text{if } \tau = 0 \\ Off_i - \delta\left(k, Off_i - l_i\right), & \text{if } \tau = 1 \end{cases} \tag{12}$$

where, τ is a random digit which takes either the value 0 or 1 and, l_i and u_i are the upper and lower bounds of Off_i. The function $\delta(k, y)$ yields a value within the range $[0, y]$ and it is designed such that the likelihood of the value being close to 0 becomes higher as k increases. The value of the function δ is given as follows:

$$\delta(k, y) = y\left(1 - \eta^{\left(1-\frac{k}{T}\right)^b}\right) \tag{13}$$

where,

- η is a uniformly distributed random number in the interval $[0, 1]$,
- k is the current generation,
- T is the maximal generation number,
- b is a system parameter determining the degree of non-uniformity.

3.3 Computation procedure for the GA Optimization

In this section, we describe the steps involved in using the proposed genetic algorithm (GA) to solve the Cauchy problem for the Helmholtz equation.
The different steps of the proposed procedure are given by:

- **Step 1 :** Parameter setting:
  - N : Population size
  - p_c : Probability of Crossover
  - p_m : Probability of Mutation
  - $MaxGen$: Maximum number of Generation
- **Step 2 :** Random generation of initial population $\phi_p^{(0)}$ with $p = 0, \cdots, N$.
- **Step 3 :** Solve the direct problem Eq.(14) below, for each given $\phi_p^{(0)}$ by the finite element method.

$$(P_{GA})_p : \begin{cases} -\Delta u + \kappa^2 u = 0 & \text{in} \quad \Omega \\ u = \phi_p^{(0)} & \text{on} \quad \Gamma_i \\ \partial_n u = g & \text{on} \quad \Gamma_c \end{cases} \tag{14}$$

- **Step 4 :** Compute the fitness value for each individual using $\mathcal{J}_{\mathcal{DR}}\left(\phi_p^{(0)}\right)$ (Eq.(7)).

- **Step 5 :** Create the next generation $\phi_p^{(1)}$ using the GA process given by:

$$\phi_p^{(1)} = M_u.C_r.S_e(\phi_p^{(0)})$$

where:

  - S_e : Random selection,
  - C_r : Arithmetic Crossover,
  - M_u : Non-uniform mutation.

- **Step 6 :** Return to step 3 and replace $\phi_p^{(0)}$ with $\phi_p^{(1)}$.

- **Step 7 :** The genetic process continue for $\phi_p^{(m)}$, $m = 1, 2, \cdots, MaxGen$.

The purpose of this procedure is to establish the Dirichlet condition on Γ_i. However, if we want to determine the Neumann condition instead, we can modify the procedure by implementing certain adjustments. Specifically, in step 2, we should replace $\phi_p^{(0)}$ with $(\phi_p^{(0)})'$ and in step 3 $(P_{GA})_p$ by $(P_{GA})'_p$ such that:

$$(P_{GA})'_p : \begin{cases} -\Delta u + \kappa^2 u = 0 & \text{in} \quad \Omega \\ u = f & \text{on} \quad \Gamma_c \\ \partial_n u = (\phi_p^{(0)})' & \text{on} \quad \Gamma_i \end{cases} \tag{15}$$

Finally, in step 4 and step 5, we need to substitute Eq.(8) for Eq.(7).

4 Numerical results and discussion

The aim of this study is to find an approximation of the missing Dirichlet and Neumann boundary conditions. Since we do not know the exact form of the solution, we will use the polynomial approximation. In order to illustrate the convergence and the stability of the proposed numerical method, we solve the Cauchy problem for the Helmholtz equation by considering two cases of domains in 2D.

The genetic algorithm used for evolving each individual population employed the following genetic operators and parameters:

- Number of Generations: $MaxGen = 200$,
- Population size: $n_{pop} = 60$,
- Crossover operator: Arithmetic Crossover, with $p_c = 0.9$,
- Mutation operator: Non-uniform Mutation, with $p_m = 0.01$,
- Insertion: We consider the principle of elitism to conserve the best solution in the next generation.

The experiments were conducted on a machine with an Intel(R) Core(TM) i7-8565U CPU @ 1.80GHz 1.99 GHz. The implementation of the algorithm was done using the software FreeFem++, [30], which is a free software for solving partial differential equations (PDEs) in $\mathbb{R}^2$ and $\mathbb{R}^3$ using finite element method. It is worth noting that the FreeFem++ language enables the rapid specification of the EDP (direct problem resulting from the considered optimization problem) by writing its variational formulation.

We investigate also the stability of the proposed algorithm by perturbing the Cauchy data f and g as follows:

$$(f_{per}, g_{per}) = (1 + \nu\theta)(f, g) \tag{16}$$

where ν denotes the noise level and θ is a random number in the range $[-1, 1]$ sampled using a uniform distribution.

4.1 First case:

In the first case, the numerical tests are made on a unit square domain $\Omega =]0, 1[^2$ (Fig.2), where the boundary $\Gamma = \partial\Omega$ is divided into two parts:

$$\Gamma_i = \{(0, y) : 0 < y < 1\}$$
$$\Gamma_c = \Gamma \backslash \Gamma_i$$

and the exact solution of the problem Eq.(1) with $k^2 = 5$ is given by:

$$u_{ex}(x, y) = \exp(2x - y)$$

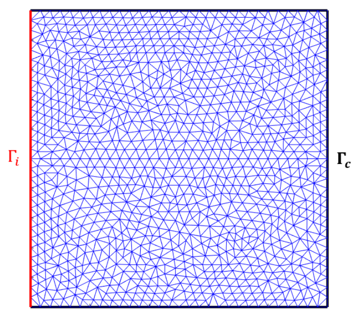

Figure 2: Unit square with mesh.

Fig.3 presents the analytical solution in the whole domain.

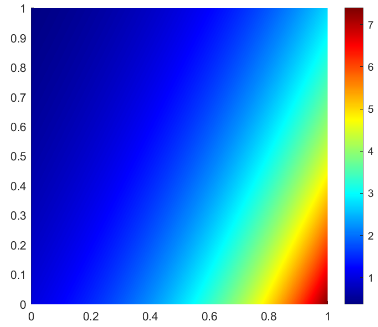

Figure 3: Analytical solution.

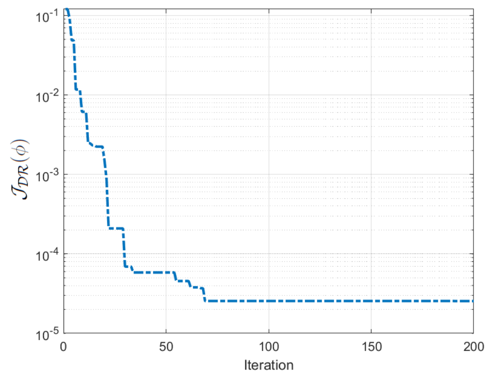

Figure 5: Objective function $\mathcal{J}_{\mathcal{DR}}(\phi)$.

4.1.1 Choice of regulation parameter

Table.[1] reveals that as the value of α and β decrease from $1e-01$ to $1e-08$, the $\mathcal{J}_{\mathcal{DR}}(\phi)$ and $\mathcal{J}_{\mathcal{NR}}(\phi')$ cost functions also decrease, indicating a better fit to the data. However, the rate of decrease slows down as we move towards smaller values of α and β, balancing the accuracy of the fit with the complexity of the solution. The results indicate that a small amount of regularization is sufficient to prevent overfitting for both $\mathcal{J}_{\mathcal{DR}}(\phi)$ and $\mathcal{J}_{\mathcal{NR}}(\phi')$, as the lowest cost is obtained for $\alpha = \beta = 1e-05$.

Fig.4 and Fig.6 illustrate the progressive convergence of the numerical solution towards the analytical solution throughout the iterative process. Initially, the numerical solution exhibits substantial deviation from the exact solution, but this discrepancy diminishes rapidly with each iteration. Such behavior highlights the efficacy of the iterative method in effectively resolving the inverse problem.

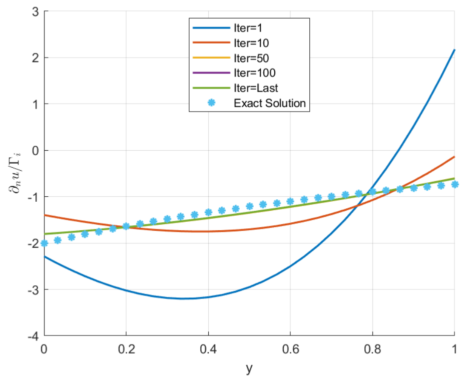

Figure 6: The derivative of u ($\partial_n u$) on Γ_i.

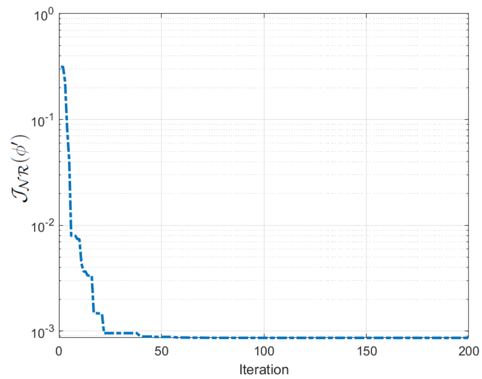

Figure 7: Objective function $\mathcal{J}_{\mathcal{NR}}(\phi')$ for different iterations.

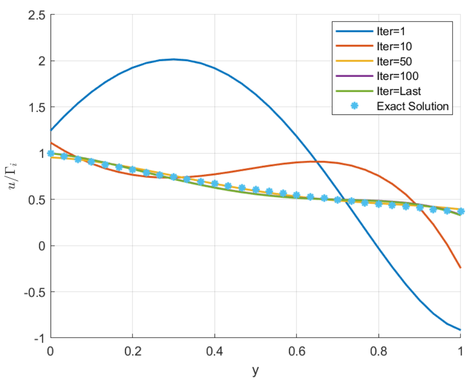

Figure 4: Trace of u on Γ_i.

Furthermore, Fig.5 and Fig.7 demonstrate the significant reduction in the objective functions $\mathcal{J}_{\mathcal{DR}}(\phi)$ and $\mathcal{J}_{\mathcal{NR}}(\phi')$ during the initial iterations. As the iterations progress, the convergence rate of the objective function gradually slows down, although it ultimately reaches a low value by iteration $k = 200$.

α and β	1e-01	1e-02	1e-03	1e-04	1e-05	1e-06	1e-07	1e-08
$\mathcal{J}_{\mathcal{DR}}(\phi)$	1.72e-02	2.09e-03	5.9e-04	1.41e-04	2.56e-05	1.31e-04	3.52e-05	6.103e-04
$\mathcal{J}_{\mathcal{NR}}(\phi')$	7.108e-02	9.31e-03	1.36e-03	6.604e-04	5.10466e-04	5.19e-04	5.201e-04	5.48e-04

Table 1: Cost function $\mathcal{J}_{\mathcal{DR}}(\phi)$ (resp. $\mathcal{J}_{\mathcal{NR}}(\phi')$) for various values of α (resp. β).

4.1.2 Stability of the Proposed Method

Fig.8 and Fig.10 illustrate a comparison between the numerical solution and the analytical solution across varying levels of noise in the measurement data. The numerical solution exhibits a slight deviation from the exact solution for low level of noise level. However, this disparity increase, when the noise level reaches a high values.

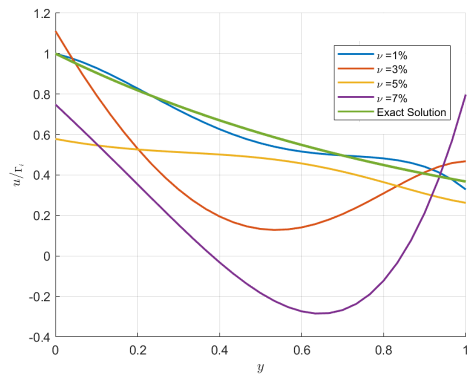

Figure 8: $u/_{\Gamma_i}$ for various levels of noise.

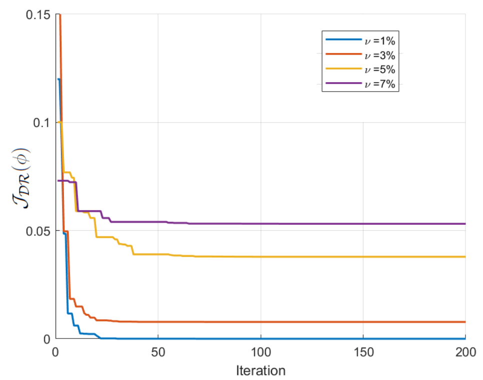

Figure 9: $\mathcal{J}_{\mathcal{DR}}(\phi)$ for various levels of noise.

In Fig.9 and Fig.11, the cost function is displayed for different noise levels, specifically $\nu = 1\%, 3\%, 5\%, 7\%$. The figures indicate that as the noise level increases, the cost function also increases, indicating a less precise fit to the data. Nevertheless, for low noise levels, the cost function remains relatively low, suggesting that the numerical solution still offers a satisfactory fit to the data.

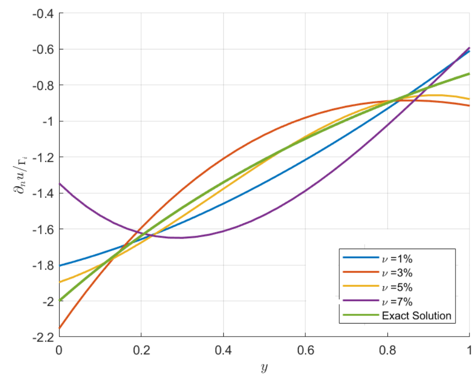

Figure 10: $\partial_n u/_{\Gamma_i}$ for various levels of noise.

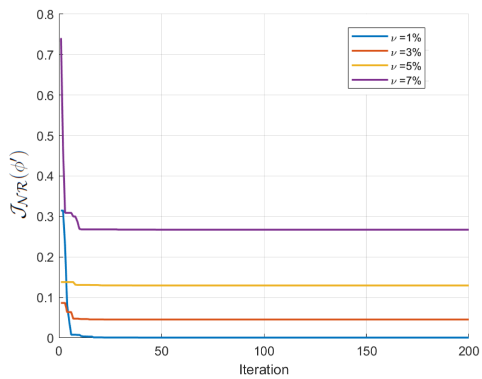

Figure 11: $\mathcal{J}_{\mathcal{NR}}(\phi')$ for various levels of noise.

4.2 Second case:

In the second case, the numerical tests are performed on an unit disc Fig.12 where the boundary of this domain is divided into two parts:

$$\Gamma_i = \Big\{(x, y) : x^2 + y^2 = 1, \quad y > 0 \quad , \quad x > 0\Big\}$$
$$\Gamma_c = \Gamma \backslash \Gamma_i$$

and the exact solution of the problem Eq.(1) with $k^2 = -2$ is given by:

$$u_{ex}(x, y) = \sin(x) \sin(y)$$

Fig.13 shows the analytical solution in the whole domain.

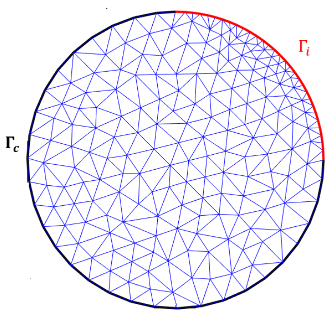

Figure 12: Unit disc with mesh.

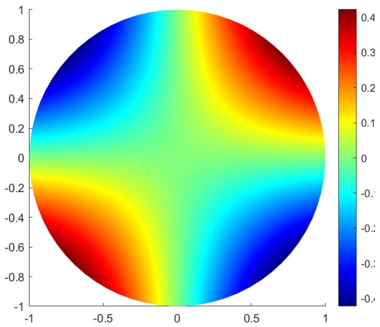

Figure 13: Analytical solution.

4.2.1 Choice of regulation parameter

Table.[2] demonstrates that reducing the value of α and β from $1e-01$ to $1e-08$ leads to a decrease in the cost functions $\mathcal{J}_{\mathcal{DR}}(\phi)$ and $\mathcal{J}_{\mathcal{NR}}(\phi')$, indicating an improved fit to the data. However, as α and β approache smaller values, the rate of decrease in the cost functions slows down, striking a balance between fit accuracy and solution complexity. These results suggest that a small degree of regularization effectively prevents overfitting for both $\mathcal{J}_{\mathcal{DR}}(\phi)$ and $\mathcal{J}_{\mathcal{NR}}(\phi')$, with the lowest cost achieved when $\alpha = 1e-04$ and $\beta = 1e-07$.

Fig.14 and Fig.16 illustrate the progressive convergence of the numerical solution towards the analytical solution throughout the iterative process. Initially, the numerical solution exhibits substantial deviation from the exact solution, but this discrepancy diminishes rapidly with each iteration. Such behavior highlights the efficacy of the iterative method in effectively resolving the inverse problem.

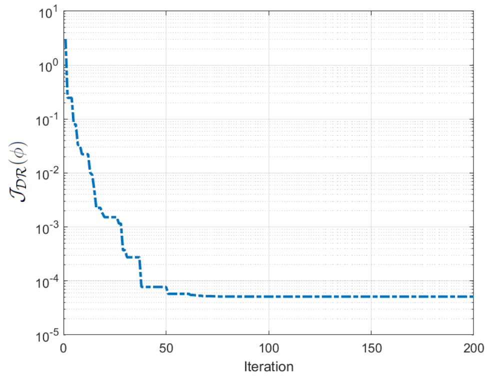

Figure 15: Objective function $\mathcal{J}_{\mathcal{DR}}(\phi)$.

Furthermore, Fig.15 and Fig.17 demonstrate the significant reduction in the objective functions $\mathcal{J}_{\mathcal{DR}}(\phi)$ and $\mathcal{J}_{\mathcal{NR}}(\phi')$ during the initial iterations. As the iterations progress, the convergence rate of the objective function gradually slows down, although it ultimately reaches a low value by iteration $k = 200$. These observations indicate that the obtained solution is highly precise and represents an excellent fit to the available data.

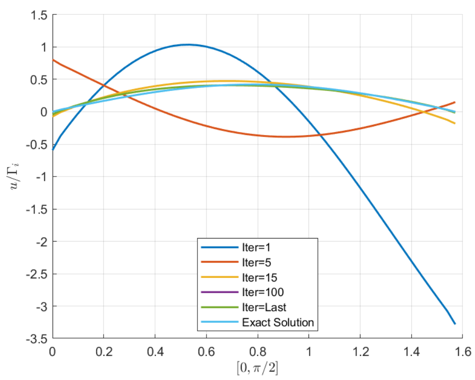

Figure 14: Trace of u on Γ_i.

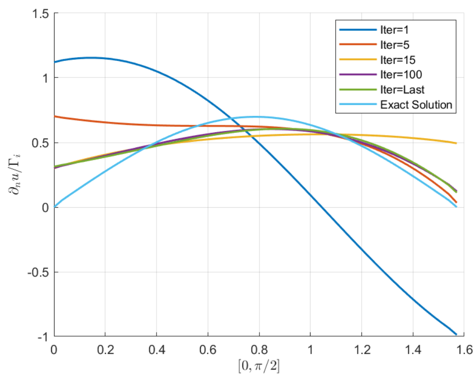

Figure 16: The derivative of u ($\partial_n u$) on Γ_i.

α and β	1e-01	1e-02	1e-03	1e-04	1e-05	1e-06	1e-07	1e-08
$\mathcal{J}_{\mathcal{DR}}(\phi)$	4.65e-03	6.69e-04	1.354e-04	2.19e-05	5.12e-05	3.574e-04	8.63e-004	5.42e-04
$\mathcal{J}_{\mathcal{NR}}(\phi')$	1.76e-02	2.12e-03	4.18e-04	6.308e-04	1.31e-03	1.07e-04	1.94e-05	1.82e-03

Table 2: Cost function $\mathcal{J}_{\mathcal{DR}}(\phi)$ (resp. $\mathcal{J}_{\mathcal{NR}}(\phi')$) for various values of α (resp. β).

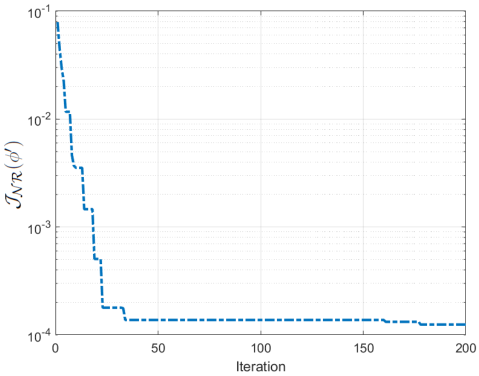

Figure 17: Objective function $\mathcal{J}_{\mathcal{NR}}(\phi')$ for different iterations.

4.2.2 Stability of the Proposed Method

Fig.18 and Fig.20 illustrate a comparison between the numerical solution and the analytical solution across varying levels of noise in the measurement data. For a low noise levels, the numerical solution exhibits a slight deviation from the exact solution. However, this disparity increase for important noise levels, in particular, when approaching Neumann condition in the extremities of the domain.

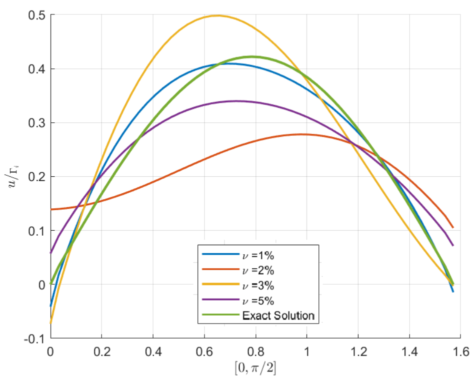

Figure 18: $u/_{\Gamma_i}$ for various levels of noise.

Fig.19 and Fig.21 depict the cost function for various noise levels, specifically $\nu = 1\%, 2\%, 3\%, 5\%$. These figures show that as the noise level increases, the cost function also increases, indicating a decreased level of accuracy in fitting the data. However, even with higher noise levels, the cost function remains relatively low, indicating that the numerical solution still provides a reasonably good fit to the data.

It is important to note that reconstructing Dirichlet boundary conditions on inaccessible parts of a boundary is typically more accurate and reliable than reconstructing Neumann boundary conditions. This is because Dirichlet boundary conditions provide more information about the solution than Neumann boundary conditions. The factors that contribute to this difference in accuracy and reliability can vary, and may depend on the geometry of the domain being studied or the regularity of the solution being reconstructed.

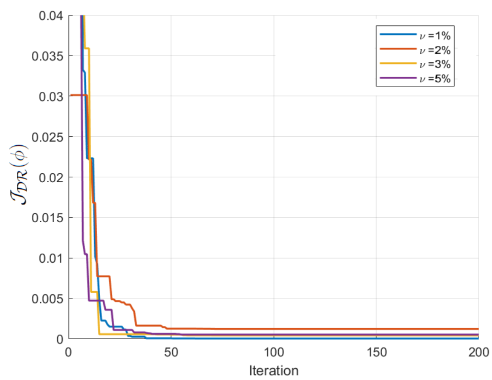

Figure 19: $\mathcal{J}_{\mathcal{DR}}(\phi)$ for various levels of noise.

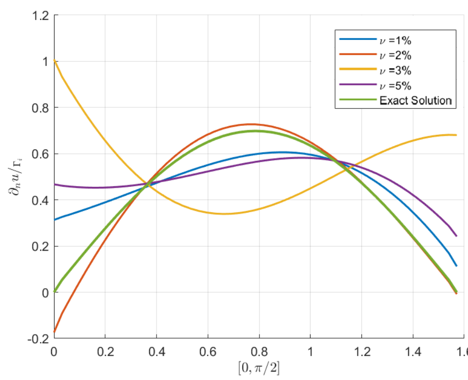

Figure 20: $\partial_n u/_{\Gamma_i}$ for various levels of noise.

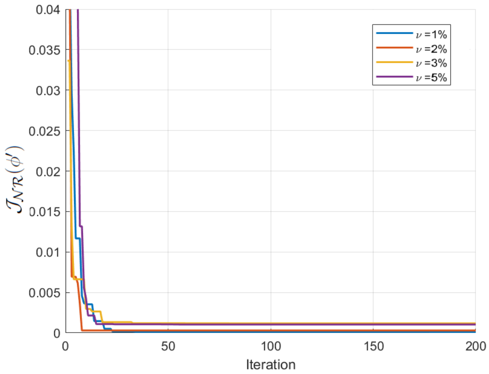

Figure 21: $\mathcal{J}_{\mathcal{NR}}(\phi')$ for various levels of noise.

5 Conclusion

In this research paper, we address the challenging ill-posed inverse problem associated with the Cauchy problem for the Helmholtz equation. Various optimization methods have been developed to approximate solutions for such problems. In this study, we explore the use of genetic algorithms, which have the advantage of not requiring specific regularity assumptions for the underlying functional. To achieve this objective, we propose an optimization formulation that incorporates a Tikhonov regularization term. The effectiveness of our approach is evaluated through numerical experiments conducted on both regular and irregular domains. The results demonstrate the efficiency of the real-coded genetic algorithm, enhanced with adapted genetic operators, in successfully solving the Cauchy problem associated with the Helmholtz equation. However, as with any other investigation, the present study has limitations related to computational complexity, the need for parameter tuning, uncertainties in solution quality, and sensitivity to initial population. These limitations create opportunities for future research exploring the utilization of parallel computing and self-adaptive algorithms.

Acknowledgment:
The authors would like to thank the editors and the anonymous reviewers for their comments and suggestions.

References:

[1] Kirsch, A. (2011). An introduction to the mathematical theory of inverse problems (Vol. 120). New York: Springer.

[2] Delillo, T., Isakov, V., Valdivia, N. & Wang, L. (2001). The detection of the source of acoustical noise in two dimensions. SIAM Journal On Applied Mathematics. 61, 2104-2121.

[3] Colton, D., Kress, R. & Kress, R. (1998). Inverse acoustic and electromagnetic scattering theory.

[4] Hall, W. S., & Mao, X. Q. (1995). A boundary element investigation of irregular frequencies in electromagnetic scattering. Engineering Analysis with Boundary Elements, 16(3), 245-252.

[5] Hadamard, J. (1923). Lectures on Cauchy's problem in linear partial differential equations (Vol. 15). Yale university press.

[6] V. Isakov, Inverse Problems for Partial Differential Equations, Applied Mathematical Sciences, vol. 127, Springer-Verlag, New York, 1998.

[7] Marin, L., & Lesnic, D. (2005). The method of fundamental solutions for the Cauchy problem associated with two-dimensional Helmholtz-type equations. Computers & Structures, 83(4-5), 267-278.

[8] Jin, B., & Marin, L. (2008). The plane wave method for inverse problems associated with Helmholtz-type equations. Engineering Analysis with Boundary Elements, 32(3), 223-240.

[9] Marin, L., Elliott, L., Heggs, P. J., Ingham, D. B., Lesnic, D., & Wen, X. (2004). BEM solution for the Cauchy problem associated with Helmholtz-type equations by the Landweber method. Engineering Analysis with Boundary Elements, 28(9), 1025-1034.

[10] Elden, L., Berntsson, F., & Reginska, T. (2000). Wavelet and Fourier methods for solving the sideways heat equation. SIAM Journal on Scientific Computing, 21(6), 2187-2205.

[11] Fu, C. L., Feng, X. L., & Qian, Z. (2009). The Fourier regularization for solving the Cauchy problem for the Helmholtz equation. Applied Numerical Mathematics, 59(10), 2625-2640.

[12] Marin, L., Elliott, L., Heggs, P. J., Ingham, D. B., Lesnic, D., & Wen, X. (2003). Conjugate gradient-boundary element solution to the Cauchy problem for Helmholtz-type equations. Computational Mechanics, 31, 367-377.

[13] Marin, L., Elliott, L., Heggs, P. J., Ingham, D. B., Lesnic, D., & Wen, X. (2004). Comparison of regularization methods for solving the Cauchy problem associated with the Helmholtz equation. International Journal for Numerical Methods in Engineering, 60(11), 1933-1947.

[14] Marin, L. (2009). Boundary element–minimal error method for the Cauchy problem associated with Helmholtz-type equations. Computational Mechanics, 44, 205-219.

[15] Yu, C., Zhou, Z., & Zhuang, M. (2008). An acoustic intensity-based method for reconstruction of radiated fields. The Journal of the Acoustical Society of America, 123(4), 1892-1901.

[16] Jin, B., & Zheng, Y. (2005). Boundary knot method for some inverse problems associated with the Helmholtz equation. International Journal for Numerical Methods in Engineering, 62(12), 1636-1651.

[17] De Jong, K. (1988). Learning with genetic algorithms: An overview. Machine learning, 3, 121-138.

[18] Kennedy, J., & Eberhart, R. (1995). Particle swarm optimization. In Proceedings of ICNN'95-international conference on neural networks (Vol. 4, pp. 1942-1948). IEEE.

[19] Socha, K., & Dorigo, M. (2008). Ant colony optimization for continuous domains. European journal of operational research, 185(3), 1155-1173.

[20] Yang, X. S., & Hossein Gandomi, A. (2012). Bat algorithm: a novel approach for global engineering optimization. Engineering computations, 29(5), 464-483.

[21] Evans, L. C. (2010), vol. 19 of Graduate Studies in Mathematics. American Mathematical Society, Providence.

[22] Vogel, C. R. (1996). Non-convergence of the L-curve regularization parameter selection method. Inverse problems, 12(4), 535.

[23] Engl, H. W. (1987). Discrepancy principles for Tikhonov regularization of ill-posed problems leading to optimal convergence rates. Journal of optimization theory and applications, 52, 209-215.

[24] Hayes-Roth, F. (1975). Review of "Adaptation in Natural and Artificial Systems by John H. Holland", The U. of Michigan Press. Acm Sigart Bulletin, (53), 15-15.

[25] Arumugam, M. S., Rao, M. V. C., & Palaniappan, R. (2005). New hybrid genetic operators for real coded genetic algorithm to compute optimal control of a class of hybrid systems. Applied Soft Computing, 6(1), 38-52.

[26] Kaelo, P., & Ali, M. M. (2007). Integrated crossover rules in real coded genetic algorithms. European Journal of Operational Research, 176(1), 60-76.

[27] Herrera, F., Lozano, M., & Verdegay, J. L. (1998). Tackling real-coded genetic algorithms: Operators and tools for behavioural analysis. Artificial intelligence review, 12, 265-319.

[28] Khouja, M., Michalewicz, Z., & Wilmot, M. (1998). The use of genetic algorithms to solve the economic lot size scheduling problem. European Journal of Operational Research, 110(3), 509-524.

[29] Michalewicz, Z. (1996). Heuristic methods for evolutionary computation techniques. Journal of Heuristics, 1, 177-206.

[30] Hecht, F. (2012). New development in FreeFem++. Journal of numerical mathematics, 20(3-4), 251-266.

Contribution of Individual Authors to the Creation of a Scientific Article (Ghostwriting Policy)
The authors equally contributed in the present research, at all stages from the formulation of the problem to the final findings and solution.

Sources of Funding for Research Presented in a Scientific Article or Scientific Article Itself
No funding was received for conducting this study.

Conflicts of Interest
The authors have no conflicts of interest to declare that are relevant to the content of this article.